JOURNAL OF PETROLOGY | VOLUME 39 | NUMBER 9 | PAGES 1669–1687 | 1998

Emplacement and Crystallization Time for the Bushveld Complex

R. GRANT CAWTHORN[1]* AND FEODOR WALRAVEN[2]

[1]DEPARTMENT OF GEOLOGY, UNIVERSITY OF THE WITWATERSRAND, PO WITS, 2050, SOUTH AFRICA

[2]924 KEYTER STREET, DASPOORT, 0082, SOUTH AFRICA

RECEIVED JULY 20, 1997; REVISED TYPESCRIPT ACCEPTED APRIL 16, 1998

The Bushveld Complex formed by the crystallization of successive injections of magma, which were sufficiently closely spaced in time that each previous magma had not cooled and differentiated significantly before the addition of the next one. To constrain the emplacement and crystallization times, a thermal model is presented which permits the investigation of the rate of cooling of magma in an intrusion repeatedly subjected to magma addition (and subtraction). Such modelling indicates that magmas injected into the Bushveld Complex were emplaced within 75 000 years. At that time injection into the Complex ceased. The volume of rock in the Eastern and Western limbs is 370 000–600 000 km^3. However, a quantitative evaluation of the Cr budget in the formation of chromitite layers indicates that large volumes of magma cannot be accounted for in the preserved rock sequence. Similarly, an evaluation of the incompatible trace-element abundances, such as those for Zr and K, suggests that the chamber was open and that large volumes of differentiated magma escaped. The volume of magma therefore greatly exceeded the preserved volume of cumulate rocks, giving an estimated magma volume of over 1 × 10^6 km^3. An average emplacement rate of 13 km^3/year is indicated by these calculations.

KEY WORDS: *Bushveld Complex; differentiation; magma emplacement rates; multiple intrusion; tapping of magma*

INTRODUCTION

The Bushveld Complex (BC) is a large layered intrusion, emplaced into a stable cratonic setting. It has been considered an intrusive equivalent of a continental flood basalt province, and inferred to be related to a mantle plume (Hatton, 1995). The duration of continental flood basaltic magmatism may be of the order of several million years. For example, the Columbia River Basalts (Hooper, 1988) were erupted in the period 17–12 Ma, with minor eruptions for a further 5 my, although most outpouring occurred within the first 2 my. It is now recognized that large intrusions were not emplaced in a single pulse, but result from multiple magma injection. The question is how rapidly were magma chambers, such as the BC, filled and how much magma was involved. Answers are relevant to the dynamics of melt production, storage and transport in the mantle and crust. This paper describes a thermal modelling technique (not previously applied to magma chambers) which can be used to analyse this process, and to obtain an estimate of the emplacement time. To present this model it is necessary to discuss the stratigraphy, size, and connectivity of the different limbs of the Bushveld Complex, and to consider the extent of tapping of the magma chamber as well as its filling.

The term 'Bushveld Complex' has been given several meanings in the literature, and according to the South African Commission on Stratigraphy (1980) includes not only the ultramafic–mafic layered rocks, but also the sills beneath the intrusion, volcanic rocks which pre-date the main mafic emplacement event, and the granitic and granophyric rocks which occur in the roof. However, in this paper the term refers only to the layered ultramafic–mafic sequence.

SETTING AND STRATIGRAPHY OF THE BUSHVELD COMPLEX

The BC was emplaced into the Kaapvaal craton at 2060 Ma (Walraven *et al.*, 1990). Generally, it was

*Corresponding author.

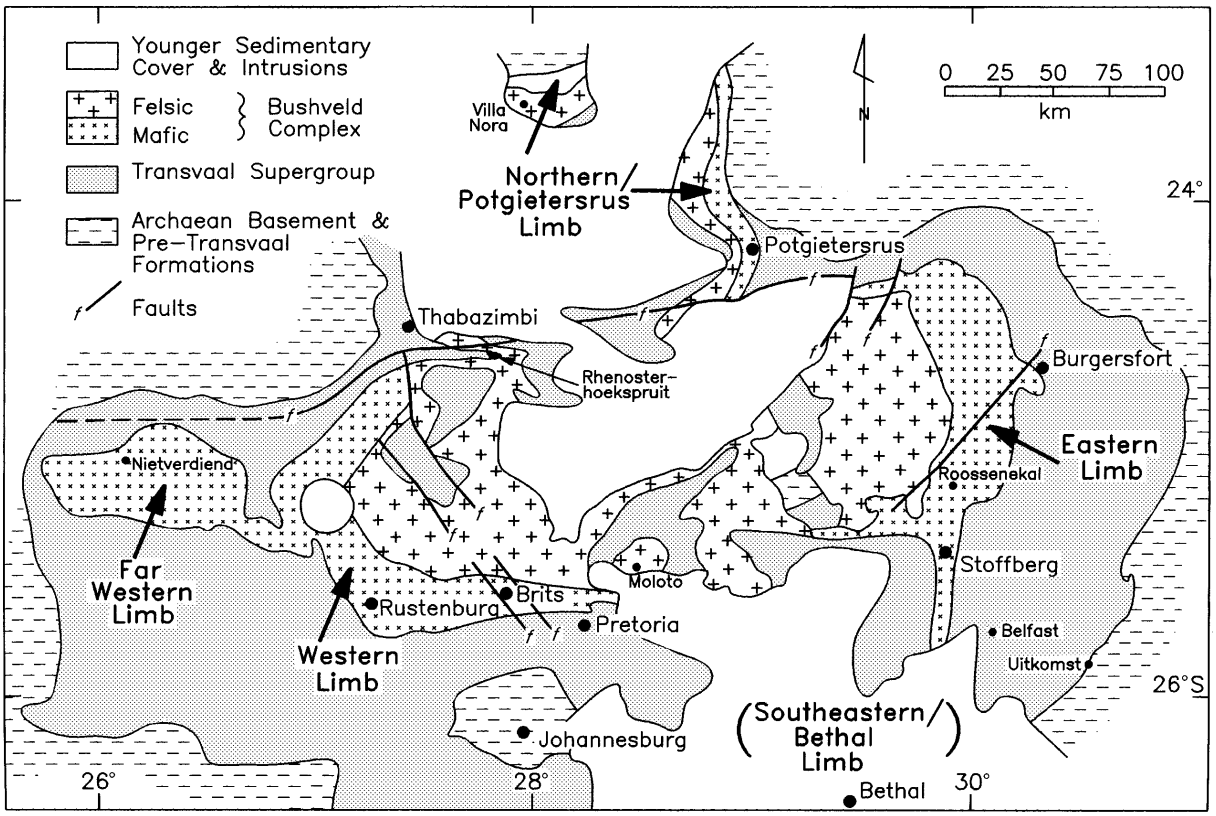

Fig. 1. General geology of the Bushveld Complex, compiled from numerous sources summarized by Eales & Cawthorn (1996).

intruded into the Transvaal Supergroup, which comprises a very thick package of intracratonic chemical and clastic sedimentary rocks, ranging in age from 2551 to 2204 Ma (Walraven *et al.*, 1990; Barton *et al.*, 1994). The general geology of the BC is shown in Fig. 1. It consists of four major limbs, the Eastern, the Western (including the Far Western), the Northern or Potgietersrus (which includes Villa Nora), and the Southeastern or Bethal limbs. Their interconnectivity is uncertain, but is discussed below. The ultramafic–mafic layered rocks can be divided into Marginal, Lower (LZ), Critical (CZ), Main (MZ) and Upper (UZ) Zones. The general stratigraphy of the two major limbs, the Eastern and Western, is shown in Fig. 2 (Eales & Cawthorn, 1996).

The Marginal Zone ranges in thickness from 0 to (in one extreme case) 800 m, consists of medium-grained norite and pyroxenite, and shows abundant evidence of crustal assimilation (xenoliths of metasedimentary rock and high modal biotite and quartz content).

The Lower Zone is poorly exposed and not continuous around the entire intrusion. In outcrop, the best exposure occurs in the Eastern limb in the Olifants River trough (Cameron, 1978), whereas a borehole drilled to the south of Thabazimbi provides a type section for the Western limb (Teigler & Eales, 1996). Rock types include pyroxenite, harzburgite and dunite (in decreasing abundance), which may be layered on scales from <1 m to hundreds of metres. Repetitive magma addition is presumed to produce the layering and oscillations in the *mg*-number [Mg × 100/(Mg + Fe)] in both mineral and whole-rock compositions (Fig. 3).

The Critical Zone has a lower pyroxenitic unit (C_LZ), within which occur numerous chromitite layers. The Upper Critical Zone (C_UZ) contains cumulus plagioclase and is cyclic, consisting of repetitions of chromitite, pyroxenite, norite and anorthosite (Fig. 3). An overall trend of differentiation can be recognized in mineral compositions (Fig. 3), although reversals also occur. In the C_UZ and above, the plagioclase and orthopyroxene may be intercumulus minerals (in pyroxenite and anorthosite, respectively), and their compositions reflect their intercumulus status. Similarly, whole-rock ratios for *mg*-number in anorthosites reflect intercumulus mafic minerals. Thus the rapid decrease in *mg*-number displayed in cycles in the C_UZ (Fig. 3) is a reflection, not of

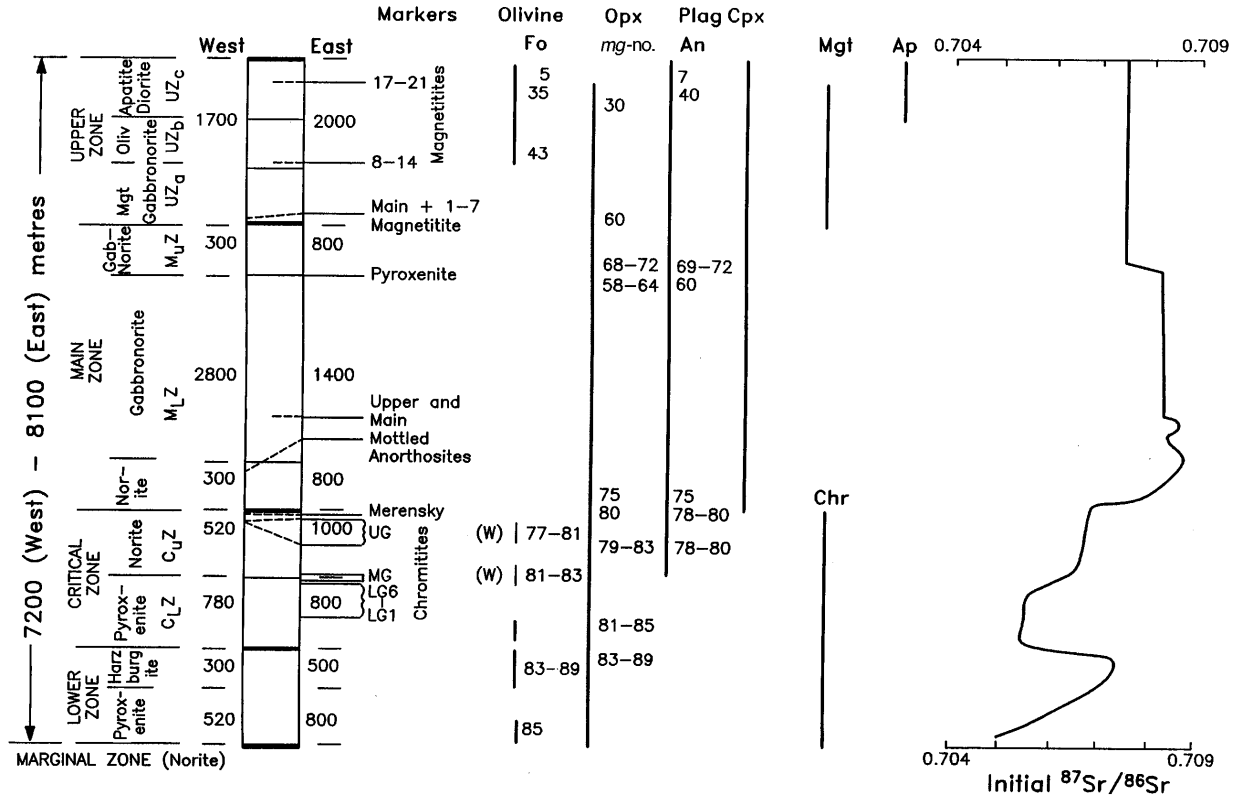

Fig. 2. Generalized stratigraphy of the Eastern and Western limbs, showing appearance of cumulus minerals and their compositions. Initial $^{87}Sr/^{86}Sr$ ratio (R_o) for whole-rock and plagioclase separates (from Kruger, 1994) is also shown. Maximum thicknesses (in m) of the Eastern and Western limbs are shown. Some of the major marker horizons are indicated with either a continuous line if they occur in both limbs or a dashed line if they are restricted to one limb. Numbers 1–7, 8–14 and 17–21 refer to clusters of magnetitite layers. This figure is compiled from numerous sources, given by Eales & Cawthorn (1996).

differentiation, but of changing cumulus status (Cawthorn, 1996).

At the level of the Merensky Reef, there is a fundamental and persistent increase in the initial $^{87}Sr/^{86}Sr$ ratio (R_o), as shown in Fig. 2 (Kruger & Marsh, 1982; Kruger, 1994), which is considered to represent a change to a new magmatic lineage dominated by plagioclase-bearing rocks. The Lower Main Zone (M_LZ) is dominated by gabbronorite with minor anorthosite. Upwards, there is a change from primary orthopyroxene to primary pigeonite (now inverted to orthopyroxene, identifiable by abundant exsolution lamellae). The An content and *mg*-number of the plagioclase and pyroxenes decrease upwards in a slow, slightly irregular, trend (Fig. 4). A dramatic increase in An content in plagioclase and *mg*-number in orthopyroxene is observed close to a marker horizon referred to as the Pyroxenite Marker (Figs 2 and 4). There is also a sustained change in R_o at this level (Fig. 2), which reflects major addition of a different magma composition. Primary orthopyroxene reappears above this break, although the major rock type is still gabbronorite.

The appearance of cumulus magnetite marks the base of the Upper Zone, but as mineral compositional trends do not show any break (von Gruenewaldt, 1973*a*; Molyneux, 1974) the combined M_UZ and UZ sequence is considered to result from normal magmatic differentiation. Numerous clustered magnetite layers occur in the UZ, and the silicate mineralogy evolves to ferrodiorite with the reappearance of olivine and later appearance of apatite as cumulus minerals (Fig. 2).

TAPPING OF THE BUSHVELD MAGMA CHAMBER

Evidence for intermittent magma addition in the BC is to be found in reversals in cumulus mineral compositions and breaks in R_o. In some intrusions 'intraplutonic quenching' has been identified and attributed to addition of magma significantly hotter than that resident in the chamber (e.g. Tegner *et al.*, 1993). The absence of such features in the BC can be construed to indicate that replenishment of magma must therefore always have

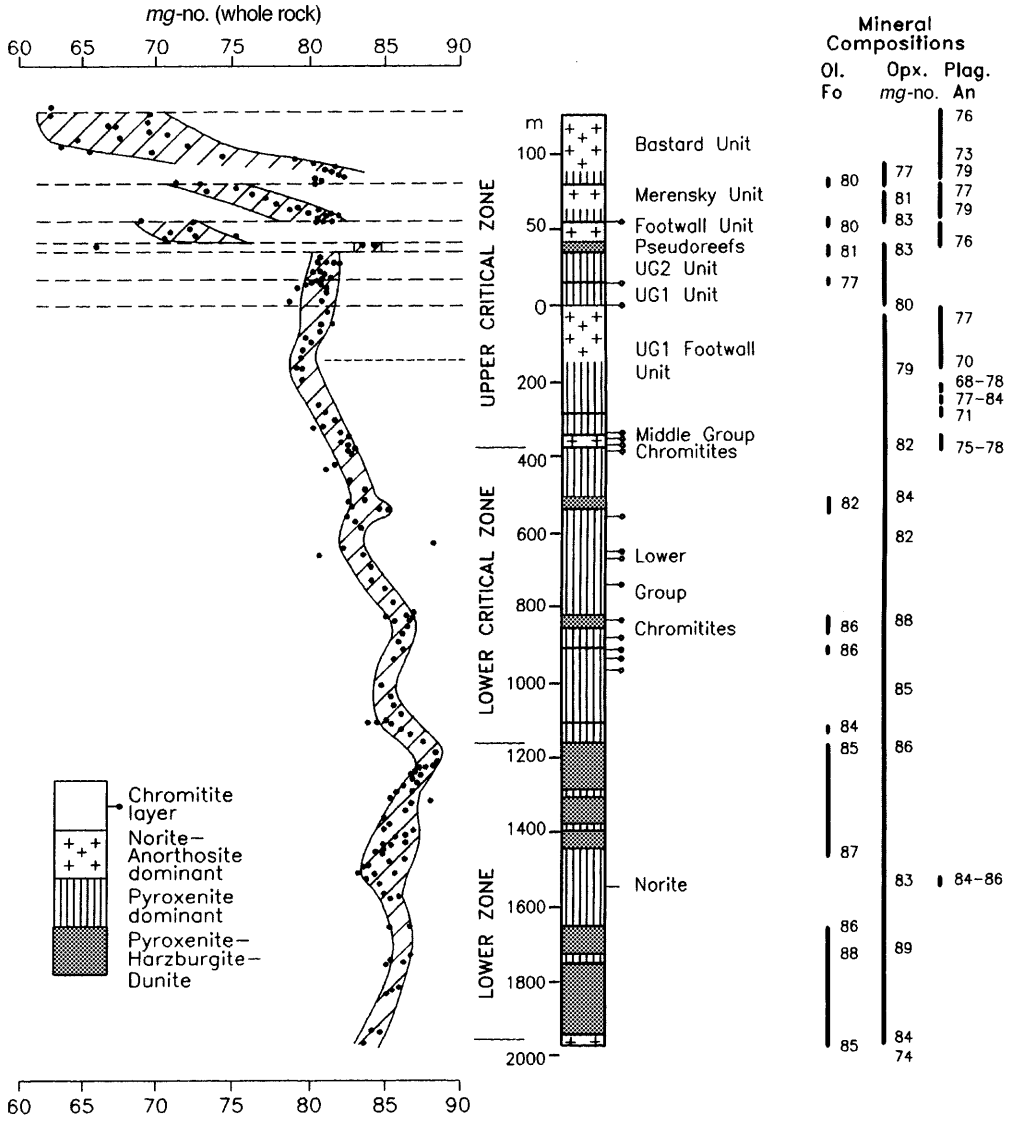

Fig. 3. Section through the Lower and Critical Zones in the Western limb showing major rock types, mineral compositions, and whole-rock *mg*-number (from Eales & Cawthorn, 1996).

occurred before the previous magma had cooled and differentiated significantly. However, what is not immediately demonstrable is whether tapping of the magma chamber occurred. It is necessary to establish the extent of this process to quantitatively model the filling and crystallization of the intrusion. Magma may have escaped from the Bushveld chamber as lava, which has now been eroded, and so indirect evidence must be sought for the operation of such a process.

The most differentiated rocks of the intrusion are diorites or ferrodiorites (von Gruenewaldt, 1973*a*; Molyneux, 1974). Nowhere does quartz attain cumulus status, and only one sample described by Molyneux from a vertical section through the entire UZ contains >2% modal quartz. Given the enormous thickness of gabbro, gabbronorite and magnetite gabbro (all of which are cumulate rocks), the absence of significant quantities of quartz-bearing differentiates suggests that at least some of the residual magma has escaped.

This problem may be addressed by estimating the bulk composition of the cumulate sequence. If the magma chamber remained closed, then the summation of all of the rock compositions in the intrusion should give the bulk composition of the magma(s). This principle was used by Wager & Brown (1968; their figs 107–109) to model the bulk composition and fractionation of the

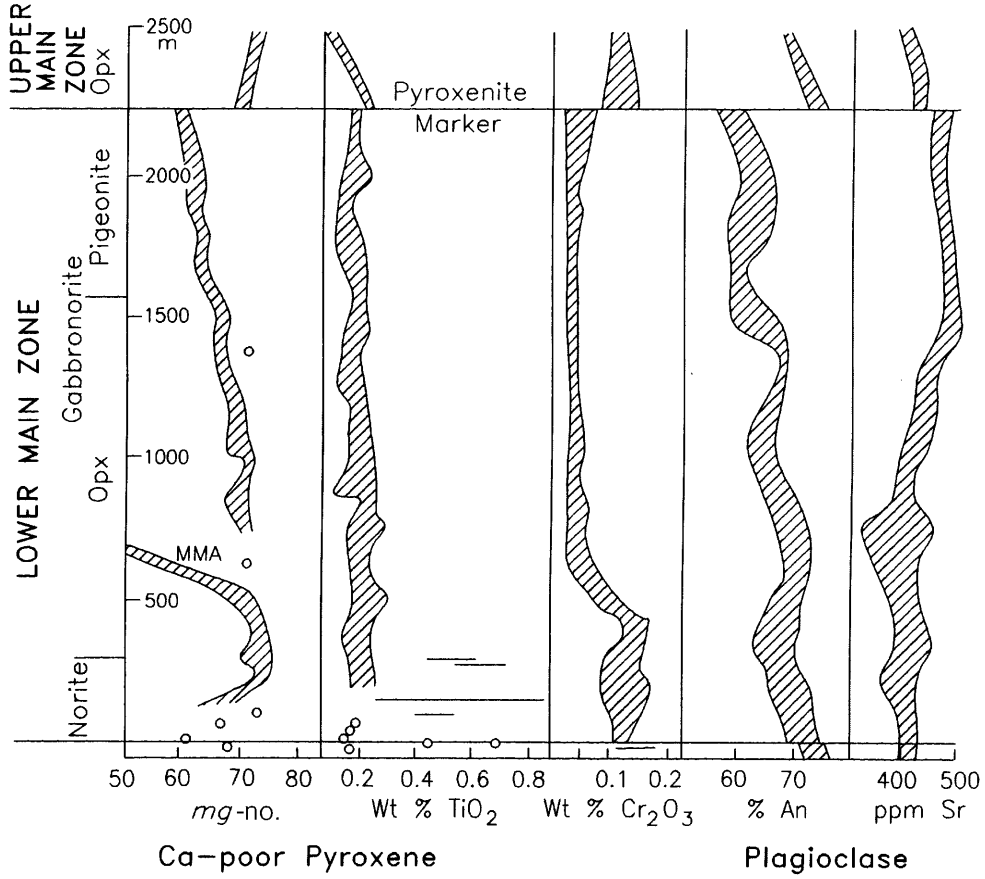

Fig. 4. Section through the Main Zone showing changing mineral compositions (from Mitchell, 1990). The shaded zone encompasses the majority of data points. Individual, isolated analyses, or where there are very few analyses, are shown as circles. A horizontal line indicates a single sample which displays a very wide range of values.

Skaergaard Intrusion. The elements Zr and K are used for the following calculation for the BC. Both elements are highly incompatible in all of the cumulus minerals in the BC. The Zr contents of samples from the different zones are shown in Fig. 5.

In the lower three major zones, the Zr values do not vary significantly or systematically as a function of height. However, in the Upper Zone there is an exponential increase in Zr with height (Fig. 5). This increase is to be expected as a result of fractionation, provided that there is no magma addition, even if Zr remains an incompatible element.

Estimates of the Zr content of the magma proposed to be parental to the Lower and Critical Zone cumulate sequences range from 35 to 70 ppm (Davies *et al.*, 1980; Sharpe, 1981). The compositions of the magmas injected at the base of the Main Zone and at the Pyroxenite Marker are harder to determine (Eales & Cawthorn, 1996), but as these are tholeiitic magmas, Zr contents are unlikely to be less than those for the ultramafic Lower Zone. The average Zr content for all of the rocks in the intrusion is far less than the average proposed magma composition, which implies that considerable volumes of evolved, and hence Zr-enriched, magma, are not represented in the preserved cumulate record. Meaningful calculations of relative volumes of cumulate to missing magma are not possible for two reasons. In determination of the average Zr content of the entire intrusion, cogniscence needs to be taken of the original area of the zones, not just their vertical heights. Estimates of areal extent are highly conjectural. Furthermore, the Zr content of the missing magma cannot be estimated.

A similar calculation can be made for another incompatible element, K. Von Gruenewaldt (1970) presented 87 analyses of Main and Upper Zone samples from the Eastern limb, which yielded an average of only 0·29% K (0·35% K_2O). Such concentrations are extremely low for a continental tholeiitic magma which is considered parental to the Main and Upper Zones (Davies & Cawthorn, 1983). These results can, therefore, be used to imply that a considerable volume of relatively differentiated magma is missing.

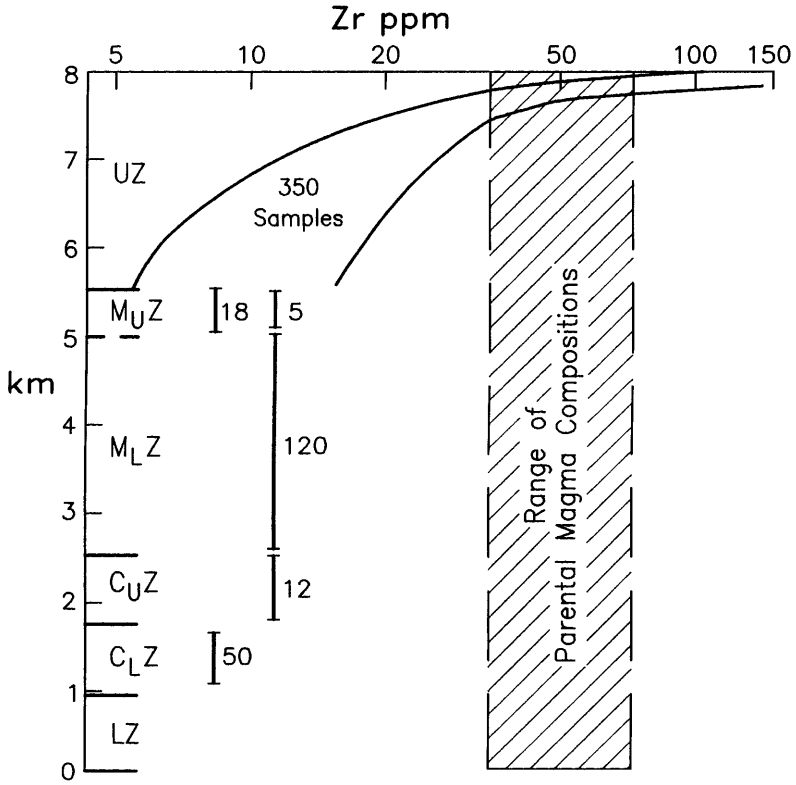

Fig. 5. Plot of Zr content (logarithmic scale) in whole-rock samples as a function of height in the BC. Average data are included for CZ and MZ, and the number refers to number of samples in each average. In the UZ the range of values is shown. Data are from Cawthorn (unpublished, 1984) for the C_LZ, Eales *et al.* (1986) for C_UZ and M_LZ, Mitchell (1986) also for M_LZ (120 samples) and M_UZ (five samples), Cawthorn *et al.* (1991) for M_UZ, and Cawthorn & McCarthy (1985; and unpublished data, 1986) for UZ. The Zr contents of magmas proposed to be parental to the LZ and C_LZ are from Davies *et al.* (1980) and Sharpe (1981).

A different type of calculation may be made for the compatible element Cr. Murck & Campbell (1986) examined a magma mixing model for the formation of chromitite layers in terms of Cr content of magmas and their temperatures. Their model is shown in Fig. 6. The magma parental to the Lower and Critical Zones (P in Fig. 6) is argued to have contained ~1000 ppm Cr (Davies *et al.*, 1980). If it is assumed that differentiated magmas resulted from 25% fractionation of olivine and orthopyroxene with a partition coefficient for Cr of three, the residual magma would have contained 500 ppm Cr (D in Fig. 6). Temperatures of 1300°C and 1200°C for the parental and differentiated magmas are likely (see below). The mixing model for chromitite layer formation would produce a liquid M (Fig. 6) which is oversaturated with respect to chromite and would precipitate chromite until the Cr content decreased to M′ (Fig. 6), a decrease of ~100 ppm. Many of the chromitite layers in the BC are 1 m thick (Hatton & von Gruenwaldt, 1987) and contain ~300 000 ppm Cr (45% Cr_2O_3). Producing a chromitite layer with this Cr content from a magma which loses only 100 ppm Cr requires the processing of a column of magma 3000 m thick. Of the seven Lower Group Chromitites, four Middle Group Chromitites and two Upper Group Chromitites, the LG6, MG1, MG4, UG1 and UG2 all approach 1 m in thickness (Hatton & von Gruenewaldt, 1987). Their formation would require a thickness of 15 km of magma for these five layers alone. The enormous lateral extent and uniformity of the chromitite layers indicates that chromite-forming events were chamber-wide phenomena and not localized, for example, mixing of magma near a feeder. It appears that there has been an extremely large volume of magma involved in the formation of the Critical Zone with its chromitite layers and that much of this has migrated laterally or vertically, and is not represented by material in the present confines of the BC.

FILLING AND COOLING OF THE BUSHVELD COMPLEX

Identifying methods of estimating the rate of filling of a magma chamber is very difficult. Lipin (1993) suggested that the Stillwater Complex could have filled at the rate of 1 km^3/year. The reversals in mineral compositions

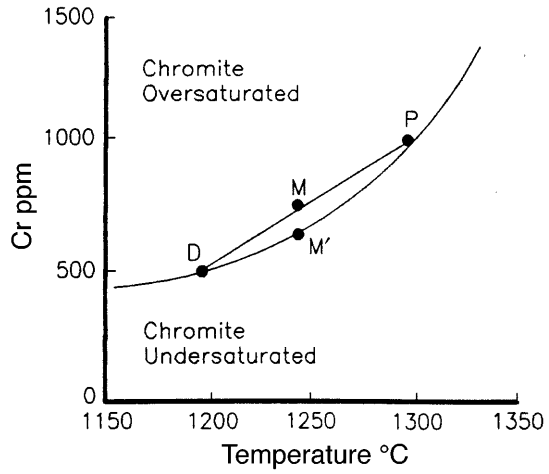

Fig. 6. Model for the formation of chromitite layers (after Murck & Campbell, 1986). The Cr contents of parental (P) and differentiated (D) magmas to the Critical Zone are indicated. The product of magma mixing is denoted by point M, and the magma composition after chromitite formation by point M′. The difference in Cr content between magmas M and M′ is ~100 ppm, and indicates how much Cr may have been extracted from the magma by the chromite-forming event.

and isotopic breaks in the BC indicate that there were distinct periods of magma addition interspersed with periods dominated by fractionation. Direct estimates of the lengths of periods of repose cannot be made, but the problem may be solved by reversing the problem and studying how quickly the magma cooled and fractionated, and determining how long it would take for a particular thickness of cumulate rocks to form between periods of magma addition.

Rates of cooling of intrusions can be modelled fairly accurately from standard heat flow equations. The two most important parameters are the thermal conductivity of country rock and thickness of magma. Jaeger's (1968) summary of models for heat flow from intrusions provides a rigorous treatment for single intrusions. Irvine (1970) developed these models further so that they were applicable to layered intrusions in which solid accumulated on the floor of the intrusion, and convection occurred within the largely liquid interior. He showed that an intrusion 7·5 km thick (equivalent to the BC) and with a liquidus temperature of 1200°C (possibly lower than current estimates) would solidify within 200 000 years. However, in neither of these formulations is it possible to add new magma, or to erupt residual magma, and so a different numerical thermal modelling technique is used here.

Cooling and crystallization model

We consider the entire crust to have been involved in the cooling process, and the crust is divided into a large number of horizontal layers of uniform thickness (Fig. 7). Each layer is assigned an initial temperature to simulate a thermal gradient. Magma is added at the required depth in the model and also divided into horizontal layers. The liquidus, solidus and emplacement temperatures of the magma need to be defined. The model is run by calculating the temperature difference between adjacent layers, and determining the heat flow and changes in heat content for a small increment of time, according to the equations

$$\Delta H = Kt(T_2 - T_1)/D$$

and

$$\Delta E = \Delta H_2 - \Delta H_1$$

where ΔH is the heat transferred from each cell to its neighbour, ΔE is the net change in heat content from one cell to the next, K is the thermal conductivity, t is the time interval, T_1 and T_2 are the temperatures of adjacent cells, D is the thickness of each cell, and H_1 and H_2 are the heat contents of adjacent cells.

New temperatures are calculated for each cell from their heat contents using different equations for the cases where the cells are totally solid, totally liquid or partially molten, e.g.

$$T = E/(CD\rho) \qquad \text{(totally solid cells)}$$

and

$$T = (E - LD\rho)/(CD\rho) \qquad \text{(totally liquid cells)}$$

where E is the heat content of a cell, C is the specific heat, ρ is the density, and L is the latent heat of solidification.

Sequential heat flow and temperature changes are calculated for successive time intervals until the total time elapsed is that required for the specific stage of the model. The pre-intrusion thermal profile would have the form shown in Fig. 7a. Immediately after magma addition the temperature profile would be that of Fig. 7b. After a period of cooling the profile would be as shown in Fig. 7c.

This calculation is an approximation, which increases in precision as the number of cells is increased, and the time interval for each step decreased. Typical values used in the models are 2000 cells over a vertical distance of 20 km (i.e. each cell is 100 m thick), and 1 year for the time interval for each step.

The advantages of this model are:

(1) a real geothermal gradient can be imposed upon the roof and floor rocks (Fig. 7a);

(2) the upper limit is the ground surface, which can be constrained to a fixed temperature;

(3) at any stage the model can be stopped and a new magma added anywhere within the crustal section (Fig. 7d);

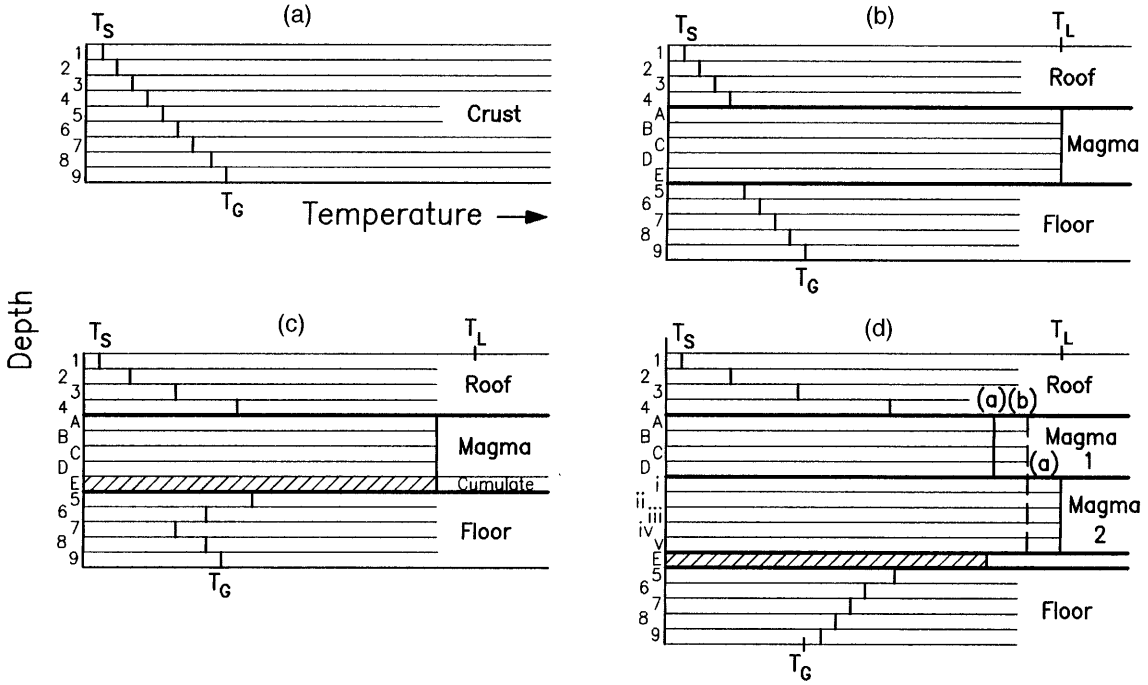

Fig. 7. Diagrammatic representation of the thermal model. (a) Pre-intrusion stage. The crust is divided into a large number of equal layers (numbered 1–9), and a thermal gradient applied, such that each layer has a distinct temperature. T_S is the temperature at the surface and T_G the temperature at depth because of the thermal gradient. (b) First intrusion. The intrusion is also divided into layers of equal thickness (denoted A–E), with a liquidus temperature of T_L. (c) Partial crystallization results in a fall in temperature below T_L, and a cumulate layer (shaded), E, forms. Roof and floor rocks heat up, giving a steeper thermal gradient in the roof and an inverted thermal gradient in the floor. (d) Second intrusion. A second magma is emplaced at the liquid–cumulate interface (i.e. between layers D and E of the first intrusion), also with a liquidus temperature of T_L, and is divided into equal layers (denoted i–v). Temperatures in the floor and roof continue to rise. It should be noted that there are two possibilities after the second injection: the two magmas may remain as thermally discrete packages (denoted a), or may mix to give a uniform temperature (denoted b). Either option can be implemented in the model.

(4) magma can either be erupted and placed at the top of the column, or totally removed (equivalent to intrusion sideways);
(5) after a small degree of fractionation, the crystalline material can be placed as a layer at the base of the intrusion (and/or at the top) with a correspondingly thinner layer of overlying liquid;
(6) added magma can be stratified within the chamber, or mixed with the residual magma;
(7) if the roof or floor rocks begin to melt, the layer of melt may be removed (extruded) or left in place;
(8) the magma chamber may be modelled as convecting or as stagnant and losing heat by conduction only.

It is therefore possible to more accurately simulate some of the processes associated with cooling and recharge of large magma intrusions.

Model for the Bushveld Complex

The application of this model to the BC requires assumptions about how much magma was added at a time, how much crystallization took place, and how much magma was erupted for each stage of the calculation. The overall model is shown in Fig. 8 and Table 1. The geological justification for these different stages is presented below.

Lower Zone and Lower Critical Zone (stages 1–6)

The LZ and C_LZ are dominated by pyroxenite, with dunite and harzburgite in the LZ, and chromitite layers in the C_LZ. The changes in mineral composition are shown in Fig. 3 and define periods where differentiation and magma rejuvenation alternate in dominance. In terms of whole-rock *mg*-number, four major periods of addition and differentiation can be recognized, but seven distinct olivine-bearing intervals are recognized. Clearly, there is not a perfect correlation between olivine-bearing rocks and high *mg*-number. Within some of the lower olivine-bearing units [well exposed in the Olifants River trough of the Lower Zone (Cameron, 1978)], dunite–harzburgite–pyroxenite units abound, with thicknesses of cyclic units of 10–20 m. Hence, it is difficult to state how many magma additions may have occurred. For these calculations, it has been assumed that there are six major

Table 1: Stages in the filling and cooling of the Bushveld magma chamber

Stage no.	Thickness magma added (km)	Thickness magma erupted (km)	Temperature of magma (°C)	Final temperature of magma (°C)	Thickness cumulate formed (km)	Total thickness cumulate (km)	Time for stage (ky)	Total time elapsed (ky)
1	1	0	1300	1200	0·25	0·25	0·25	0·25
2	1	0	1300	1200	0·25	0·5	1·1	1·3
3	1	0·25	1300	1200	0·25	0·75	2·0	3·3
4	1	0·25	1300	1200	0·25	1	2·9	6·2
5	1	0·25	1300	1200	0·25	1·25	3·6	9·8
6	1	0·25	1300	1180	0·35	1·6	9·2	19
7	8	8	1300	1150	0·8	2·4	13	32
8	3	2	1160	1140	0·8	3·2	8	40
9	1·5	1	1160	1130	0·6	3·8	9	49
10	1·5	1	1160	1120	0·6	4·4	12	61
11	1·5	1	1160	1110	0·6	5·0	16	77
12	1·5	1	1200	1100	0·5	5·5	24	101
13	0	0·5		1025	1·2	6·7	39	140
14	0	0·5		900	0·8	7·5	40	180
		0·5						

periods of addition of magma. The orthopyroxene varies from a maximum of En_{89} to En_{82} within this interval (Fig. 3). The experimental data of Cawthorn & Biggar (1993), who studied the melting relations of magma proposed to be parental to the BC, can be used to translate mineral compositions into temperatures and extent of differentiation. The relationship between temperature and En content of the orthopyroxene is shown in Fig. 9. Starting with a magma with 11% MgO, which will crystallize orthopyroxene En_{89} at 1300°C, it can be calculated that 25% crystallization will produce a residual magma with 7% MgO which will crystallize En_{82} at 1200°C. The typical thickness of the ultramafic package of the LZ and C_LZ is ~1·5 km (Fig. 2). Hence, 6 km of magma is required to produce this thickness of cumulate rocks, and so six pulses of magma each 1 km thick are used in the model.

In running the model, it was assumed that the magma cooled repeatedly to 1200°C and produced En_{82} each time, although such extreme compositions are not always identified in the actual profile (Fig. 3). Added magma is assumed to have mixed with the resident magma and so combined magma temperature fell with each addition as shown in Fig. 8. It is considered unlikely that a magma chamber relatively close to the surface could inflate to 6 km in thickness without rupturing and erupting through its roof, and so with magma additions 3–6 it is assumed that 0·25 km of magma leaked from the system, either vertically or horizontally. This leakage has the effect of decreasing the total thickness of the magma column. At the end of stage 6, the magma chamber contained 1·5 km of cumulate rocks and 3·5 km of overlying magma.

Upper Critical Zone (stage 7)

The base of the C_LZ is taken at the appearance of cumulus plagioclase. The coexisting orthopyroxene had a composition of En_{80} (Figs 2 and 3), corresponding to a temperature of 1180°C (Fig. 9). To reach these conditions, the sixth stage was allowed to continue to these lower temperatures as shown in Fig. 8.

The C_LZ is one of the most remarkable sequences in the BC, consisting of approximately eight cyclic units ranging from chromitite, through pyroxenite to norite and anorthosite. However, each cycle is thin and the total package is <800 m thick (Fig. 3). The mass balance calculations presented above for Cr show that to produce chromitite layers up to 1 m thick an enormous volume of Cr-rich magma must have been repeatedly introduced during the formation of the C_UZ. This sequence is therefore modelled by eight additions of magma, each 1 km thick, and each crystallizing 100 m of cumulate rocks. However, these additions would build up a liquid column over 10 km thick, which is considered unrealistic, and consequently differentiated magma is assumed to have leaked from the system, restricting inflation of the chamber. Stage 7 is modelled therefore by eight identical repetitive additions of 1 km of primitive magma and withdrawal of 1 km of residual magma. At the end of

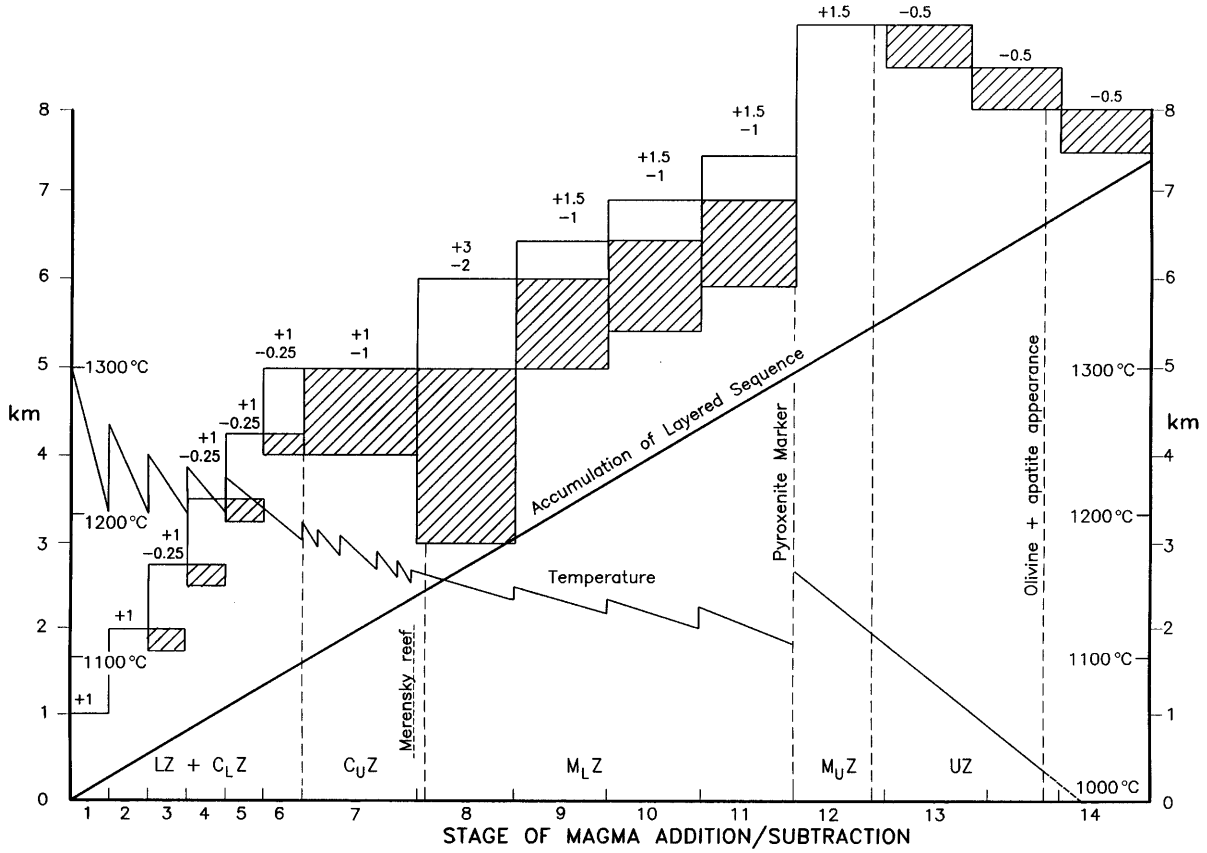

Fig. 8. Diagrammatic model for the filling and crystallization of the BC. The process is divided into stages (along the horizontal axis), which represent addition and/or subtraction of magma (see Table 1). The vertical axis represents thickness both of magma and cumulate rocks, and is also a temperature axis. The diagonal line through the diagram shows the thickness of cumulate rocks formed. At each stage the volume of magma added and subtracted is shown. Subtraction is shown by the shaded box. Numbers indicate the thickness of magma added and/or subtracted in km, e.g. +1, –0·25 means that 1 km of magma was added and 0·25 km of residual magma was removed. The different zones of the BC are indicated along the base of the diagram.

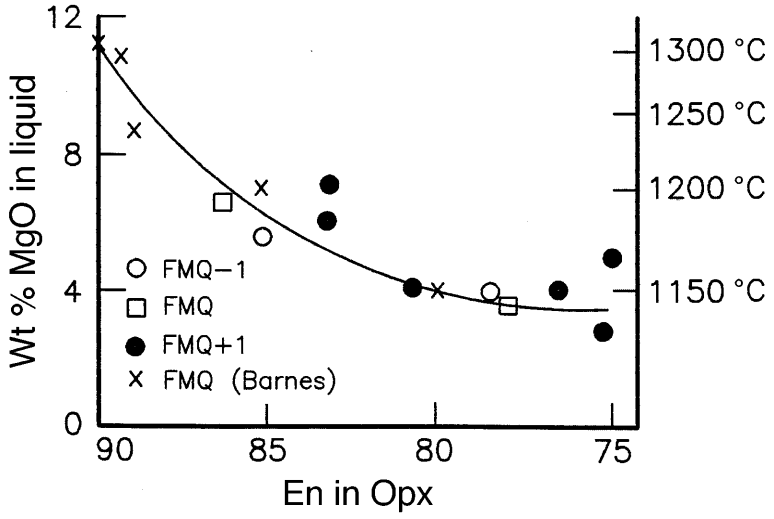

Fig. 9. Plot of orthopyroxene compositions as a function of temperature, oxygen fugacity, and approximate MgO content of the magma [based on experimental data of Barnes (1986) and Cawthorn & Biggar (1993)].

the stage, the temperature had fallen to 1160°C, consistent with the most evolved cumulus orthopyroxene compositions of En_{77}.

Lower Main Zone (stages 8–11)

The base of the MZ is traditionally taken as the top of the last cyclic unit that ranges from chromitite to anorthosite, which occurs at the top of the Bastard Cyclic Unit (Fig. 3). However, from the R_o data, the major break occurs at the Merensky Reef, where there is an abrupt increase in R_o from 0·7063 to 0·7075 over a few metres, and it continues to increase to 0·7085 within 200 m. Thereafter, R_o remains virtually constant throughout the entire 2 km of the M_LZ (Fig. 2). The compositions of the plagioclase and orthopyroxene evolve extremely slowly with increasing height from An_{73} to An_{60}, and from En_{73} to En_{60} through this interval (Fig. 4), with subtle reversals (von Gruenewaldt, 1973*a*; Mitchell, 1990). These observations place major constraints on the nature and volume of magma batches entering and escaping from the chamber. The isotopic data indicate that the magma entering the system at the Merensky Reef level was different from that which produced all the previous cumulate rocks. From the mineral compositional data it is inferred that the new magma was fairly evolved (Cawthorn, 1996). If magma was intermittently added during crystallization of the MZ and mixed with a significant volume of residual magma complementary to the C_UZ cumulate rocks, the isotopic ratio would steadily increase upwards throughout the entire M_LZ. The fact that the ratio remains constant suggests that this model is not correct. The constancy of the isotopic ratio suggests instead that most of the residual magma from the CZ was displaced from the chamber, such that there was minimal residual magma left to mix with the multiple additions of MZ magma. This model is substantiated by the constant R_o in MZ cumulate rocks.

Stage 8, which represents the transition from the Merensky Reef into typical MZ rocks, has been modelled, therefore, by the expulsion of 2 km of residual magma and addition of 3 km of new magma with a liquidus temperature of only 1160°C, consistent with the evolved mineral compositions. Further additions of 1·5 km of isotopically identical magma, and expulsion of 1 km of residual magma occurred for stages 9–11, and result in the very slow differentiation observed through this subzone. The *mg*-number of the pyroxenes and the An content of the plagioclase decrease by ~10% through the M_LZ (Figs 2 and 4). Yang *et al.* (1996) showed that changes in composition from An_{70} to An_{60}, and corresponding changes in the pyroxene, require ~60% crystallization and a temperature decline from 1170°C to 1110°C. This final temperature of 1110°C is also consistent with the experimental data of Snyder *et al.* (1993) and Toplis & Carroll (1995), who showed that magnetite appears at ~1100°C in typical tholeiitic magmas. Comparison of mineral compositions at the base of the UZ, where magnetite becomes a cumulus mineral, with those at the level immediately below the Pyroxenite Marker (Fig. 2) indicates that the magma was close to magnetite saturation at this level but its appearance was delayed by magma addition.

Upper Main Zone and Upper Zone (stages 12–15)

Reversals in mineral composition and a major, sustained change in R_o close to the level of the Pyroxenite Marker indicate addition of magma at this level. The increase in An and En values of 10% in mineral compositions crystallized from the mixed magma (von Gruenewaldt, 1973*a*; Sharpe, 1985; Cawthorn *et al.*, 1991) indicates emplacement of a new magma significantly hotter and more primitive than the residual magma, and a temperature for the new magma of 1200°C is assumed in the model. Von Gruenewaldt (1973*b*) suggested that there was 2 km of magma left in the chamber at the Pyroxenite Marker, and that 1 km was added, these data being based on models of differentiation. In the present model it is assumed that there was 2·5 km of magma left in the chamber at the end of stage 11, and that 1·5 km of magma was added. As the residual magma was at a temperature of ~1120°C, the mixed magma would have a temperature of 1150°C. Both von Gruenewaldt (1973*a*, 1973*b*) and Molyneux (1974) concluded that from the Pyroxenite Marker to the top of the UZ there was uninterrupted differentiation. This suggestion is supported by the Sr isotopic data of Kruger *et al.* (1987), which show absolutely constant values throughout this 2·5 km thick succession. The inference that 4 km of magma produced only 2·5 km of cumulate rocks requires that 1·5 km of residual magma was lost from the chamber, which is consistent with the mass balance considerations for Zr and K discussed above, where expulsion of differentiated magma was proposed.

The subdivision of the BC into the various stages listed above is justified and well constrained on the basis of cyclicity, mineral compositional variation, and R_o patterns. However, the exact number of injections of magma which built up these stages cannot be quantified, and the precise number of injections used in the models should not be considered absolute. The total thickness of magma required during each stage is, however, well constrained by geochemical and mineralogical data.

Time scale for crystallization

Using the iterative model described above, it is possible to add and subtract the various thicknesses of magmas with the temperatures indicated in Table 1 and to predict

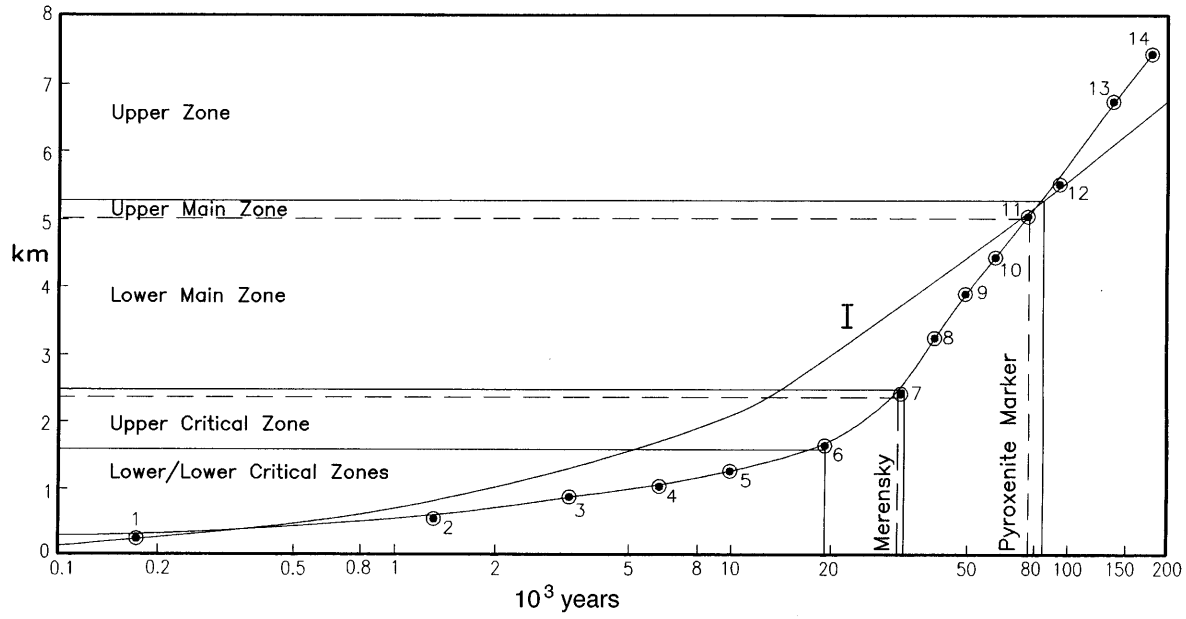

Fig. 10. Crystallization time for the BC based on the magma injection model of Fig. 8. For comparison, the crystallization time for a 7·5 km thick, single injection of magma (Irvine, 1970) is shown (curve denoted I).

crystallization times. For each stage, the initial and final temperatures, and the thickness of magma are the important parameters, and these are constrained by mineral compositions and appropriate experimental data.

Stage 1 involved the addition of 1 km of magma at 1300°C at a depth of 3 km below surface. It cooled to 1200°C, and underwent 25% crystallization, producing 0·25 km of cumulate rocks, before the next addition of magma (Table 1). This relatively thin body cooled quickly and the stage was completed in 250 years (Fig. 10). Successive stages took much longer as the chamber became thicker, and the country rocks were heated. The ultramafic sequence (stages 1–6) of LZ and C_LZ formed in ~19 000 years (Fig. 10).

Stage 7 and all subsequent stages involved the crystallization of several minerals including plagioclase. Along such cotectic curves, a given proportion of fractionation occurs with a much smaller fall in temperature than along the orthopyroxene-dominated liquidus surface along which the LZ and C_LZ were produced. Hence, a greater thickness of cumulate rocks forms in the C_UZ and above than in the ultramafic sequence for a given fall in temperature, and so the rate of accumulation increased above this horizon even though the rate of heat loss was decreasing (see Fig. 10). Accumulation to the top of the C_UZ was achieved ~30 000 years after the onset of magmatism.

The thermal gradients in the immediate floor and roof rocks to the BC steadily declined as crystallization proceeded and they heated up, so the rate of heat loss decreased. Consequently, the rate of cooling of the magma continuously decreased and accumulation rates decreased. The M_LZ took about a further 45 000 years to accumulate, and the M_UZ and UZ a further 100 000 years. As the solidus temperature of the differentiated tholeiitic magma is difficult to predict, especially in terms of the effects of water pressure, the final solidification time cannot be predicted accurately, and so this last figure cannot be considered very reliable.

It was shown above that the level of the Pyroxenite Marker represents the last addition of magma. The constancy of R_o and the regular differentiation shown by mineral compositions above this level attest to the termination of magma addition. Hence, the BC was intermittently replenished for ~75 000 years, and thereafter magma addition ceased.

These results can be compared in Fig. 10 with the data of Irvine (1970), who modelled the crystallization times of large intrusions, assuming a single injection of magma. The overall times for formation of a 7·5 km thick intrusion are similar for the two models. This is to be expected, as comparable heat content of the magma had to be expelled from the intrusion through the country rocks. Thermal diffusion in solid rock being so slow, it is the rate-determining process for cooling. However, major differences in the accumulation rate between the two models are apparent in Fig. 10. Specifically, in the LZ and C_LZ, and up to the level of the Merensky Reef (stage 7), the accumulation rate in the present model is slower by a factor of at least three than in the single

injection model. This difference is the consequence of two effects. Hot (1300°C) magma was added and progressively a greater volume of cool (1200°C) magma was expelled. Hence, the overall temperature of the magma was kept higher in the multiple intrusion model. Further, initially a large temperature fall is required for a small percent of orthopyroxene crystallization, whereas once magmas become saturated with several minerals, a small decrease in temperature causes a greater percent crystallization. In Irvine's model, the percent crystallization was a linear function of temperature from liquidus to solidus. In the present model it is possible to determine more accurately the time interval between successive pulses of magma, provided that there is sufficient information on the change in mineral compositions, and hence the temperature decrease, between each injection.

VOLUME OF THE BUSHVELD MAGMA CHAMBER

It is difficult to estimate the total volume of magma which produced the mafic rocks of the BC. The main uncertainties are:

(1) the original lateral extent of the intrusion beyond present erosional limits;
(2) whether each lobe was strictly synchronous and/or physically connected;
(3) the variability of thickness;
(4) whether there was eruption from the chamber.

Each of these aspects is discussed below.

Area

The present outcrop of the BC can be divided into four major limbs (Fig. 1). The outcrop of the Western limb is almost semi-circular with a radius of 60 km, and dips are of the order of 10–15°C centripetally. There is an extension which has been referred to as the Far Western limb and was probably contiguous with the Western limb before erosion. The Eastern limb is a mirror image of the Western limb, but has an extension southwards which is hidden below younger sedimentary rocks to the south. Based on gravity data and subsequent drilling, it has been shown that a sizeable layered mafic sequence occurs further to the south of this extension. It is known as the Bethal lobe, and original continuity between it and the Eastern limb was probable. The Northern or Potgietersrus limb has two exposures, one as a north-trending, 90 km long body, and a second as an equant exposure 50 km further west. However, these two are almost certainly contiguous beneath the younger sedimentary cover (Fig. 1). The geometrical relationships between the Northern and Eastern lobes are also hidden under younger cover, where the two are separated by the Thabazimbi–Murchison Lineament, which can be traced from Thabazimbi, eastwards, to immediately south of Potgietersrus (Fig. 1). As some of the movement along this sinistral fault zone post-dated the emplacement of the BC (du Plessis & Walraven, 1990), it is probable that these two lobes were also originally contiguous.

Between the Western and Eastern lobes are isolated occurrences of layered rocks. Extensions to the Western lobe can be seen at Rhenosterhoekspruit, east of Thabazimbi (Fig. 11a) where 1·5 km of Upper Zone rocks with magnetite layers has been identified, and at Moloto east of Pretoria (Fig. 1) where again Upper Zone rocks have been intersected in bore-core (Walraven, 1987). In the Eastern limb, an isolated dome at Malope (Fig. 11a) exposes C_LZ to UZ rocks (Marlow & van der Merwe, 1977). The similarities between rocks at these three localities with sections of the Bushveld stratigraphy in the Eastern and Western limbs strongly supports the concept of lateral continuity with these two main limbs.

Evidence for a greater lateral extent of the original chamber than its present limits can be found from a variety of geological information. Metamorphism of the floor rocks (mainly the Transvaal Supergroup) can be traced well beyond the present erosional limits of the intrusion and can be regarded as evidence for lateral extension. These metamorphic limits are shown in Fig. 11a. Around the Eastern limb, they have been precisely defined by Button (1976). In the Far Western and Western limb the presence of andalusite- and cordierite-bearing rocks has been reported by Engelbrecht (1976) and Davies (1980), respectively. The limits of observable mineralogical metamorphic change on surface do not define the limit of the Bushveld chamber. They merely indicate that the dip of these floor rocks is such that, beyond these limits, the chamber was at a level so far above these rocks that the effect of metamorphism was minimal. Hence, these metamorphic limits define a minimum extension to the Bushveld chamber.

In the Eastern Bushveld a gravity and magnetic survey by Molyneux & Klinkert (1978) indicated the probable westwards extent of the intrusion. These workers defined a limit of magnetite-rich rocks based on magnetic anomalies, which is shown in Fig. 11a. Gravity surveys by these workers and Hattingh (1980) have also been used to infer extensions down-dip. Such gravity interpretations are model dependent and become less reliable with increasing depth when traced westwards, but are also shown in Fig. 11a. A cross-section based on the interpretation of the geophysical data is shown in Fig. 11b. Gravity studies in the west by Walraven & Darracott (1976) and du Plessis & Kleywegt (1987) also indicate that mafic rocks may underlie the entire semi-circle from Thabazimbi to Pretoria.

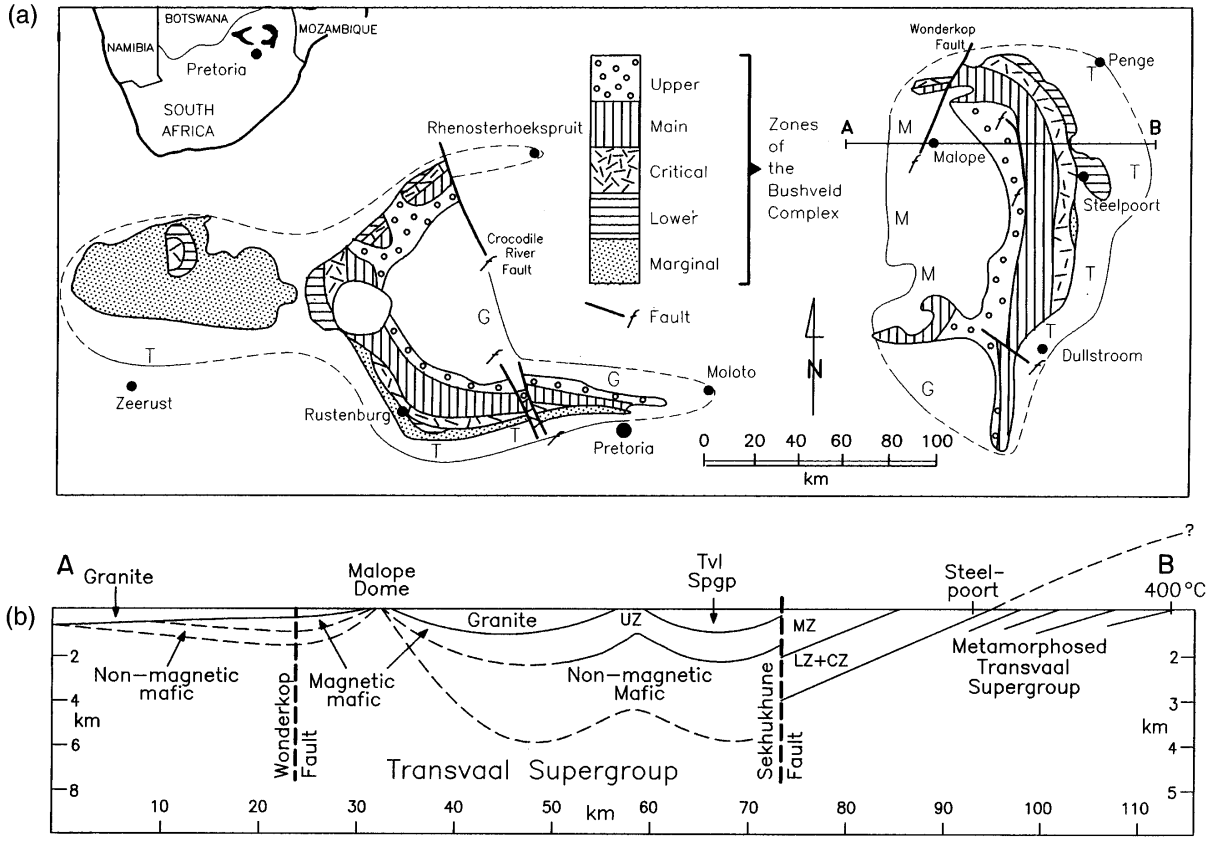

Fig. 11. Evidence for the extension of the BC beyond its present erosional limits. (a) Evidence from thermal metamorphism of the floor rocks is shown by the symbol T, from magnetic data shown by M, from gravity data shown by G, and from isolated exposure or bore-core information at Moloto and Rhenosterhoekspruit. Where specifically studied, the limit of metamorphism is shown by a continuous line, and where inferred it is shown by a dashed line. The line of the cross-section (AB) in (b) is indicated. (See text for sources of information.) (b) West–east cross-section through the Eastern Bushveld (from Molyneux & Klinkert, 1978). The macroscopically delineated limit of contact metamorphism approximates to the 400°C isotherm (Button, 1976), and is shown at the east end of the section. Rock types 'magnetic mafic' and 'non-magnetic mafic' are inferred from the combined magnetic and gravity models, and are equivalent to the UZ and all other zones of the BC combined, respectively. 'Tvl Spgp' refers to a raft of Transvaal Supergroup rocks, which are important in the gravity modelling but are not shown in (a).

Synchrony

Isotopic dating indicates that all lobes are synchronous within the limits of error, and so all are justifiably regarded as part of the BC (Walraven *et al.*, 1990). However, they may either be synchronous, implying simultaneous filling of all limbs of the entire intrusion, or sequential, suggesting a more prolonged period of episodic emplacement, analogous to that observed in the Duluth Complex (Miller & Ripley, 1996). The fact that comparable sequences of rock types and mineral compositions occur in many of the limbs does not prove consanguinity and/or physical connectivity. The principles of magmatic differentiation dictate that magmas of similar composition must evolve through comparable differentiation sequences, regardless of their age. This feature is well demonstrated in the Duluth Complex, where broadly similar sequences of rocks are recorded from different bodies which have discordant relations to one another (Miller & Ripley, 1996). Hence, it is the evidence from anomalous horizons or sequences of rocks, which are not predictable from normal magmatic fractionation and occur in more than one limb, that must be examined to demonstrate physical connectivity. Several mineralogically and/or geochemically distinct horizons, which show remarkable similarity within the Eastern and Western limbs, can be documented. Their stratigraphic positions are shown in Fig. 2.

Middle Group Chromitites

The transition from the C_LZ to the C_UZ is defined by the appearance of cumulus plagioclase. Four chromitite layers straddle this boundary, and are collectively referred to as the Middle Group Chromitites. One occurs in the footwall pyroxenite, the second occurs exactly at the contact of pyroxenite with the lowest anorthosite layer and two occur slightly above (Fig. 12) this contact. These

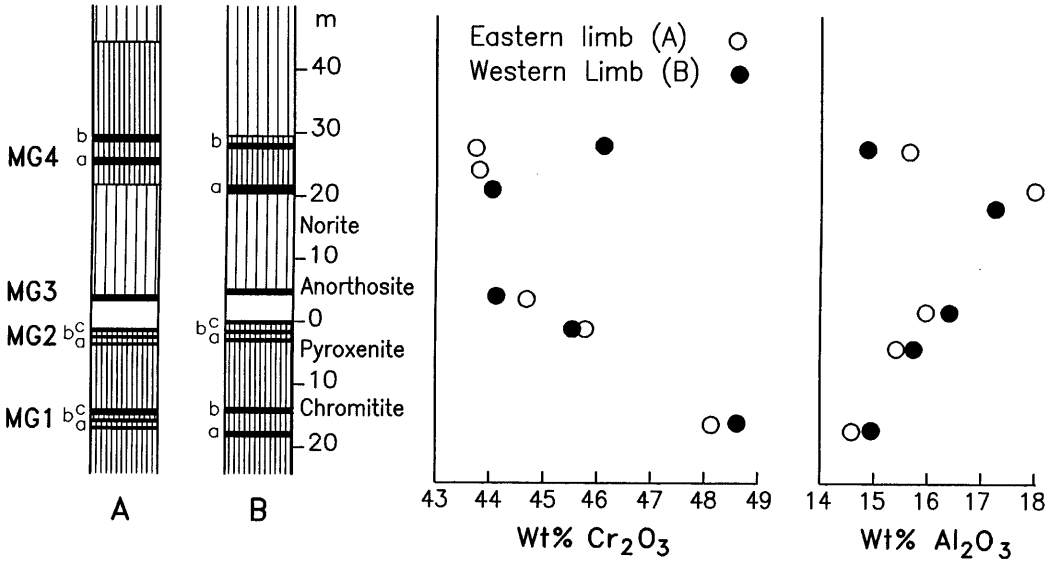

Fig. 12. Section through the Middle Group Chromitites in the Eastern and Western limbs. The sections and the chemical compositions of the chromitite layers are taken from Hatton & von Gruenewaldt (1987).

layers are usually composite and consist of two or three discrete layers occurring very close together. The Middle Group Chromitite sequence is about 45 m thick in both Eastern and Western limbs. There is a considerable vertical sequence above and below this package of rocks devoid of chromitite layers. Multiple chromitite layers cannot be attributed to normal fractionation processes within a single magma, and so the similarity between these two sequences suggests that both limbs were simultaneously affected by the same chromite-forming events. Each chromitite layer has its own unique chemistry, and compositions tend to evolve uniformly upwards. The compositions of each of the Middle Group Chromitite layers from both the Eastern and Western limbs are shown in Fig. 12. The chemical similarity between the layers in the east and west, with the possible exception of the Cr_2O_3 content of layer 4b, is remarkable, and again suggests that these are part of originally continuous layers.

Upper Group Chromitite Layer 1

The Upper Group Chromitite 1 (UG1) is very distinctive in being disrupted in a variety of ways. It shows extensive bifurcations, encloses numerous lenses of anorthosite, is disrupted by discordant anorthosite bodies, and shows folding and deformation (Lee, 1981). These features (so well exposed at Dwars River) can be observed wherever the UG1 is exposed in both the Eastern and Western limbs, especially in all mining activities through this section. These post-depositional features are not observed in any other layer and suggest a unique event. We conclude that the UG1 layer was continuous from the Eastern to Western limbs.

Merensky Reef

The Merensky Reef cyclic unit is a short vertical interval of rocks with very distinctive features, which cannot be attributed to differentiation within a single magma. The R_o increases dramatically across this unit from 0·7064 to 0·7074 in both Eastern and Western limbs (Kruger & Marsh, 1982; Lee & Butcher, 1990). The grades of platinum mineralization are extremely similar. Such similarity of two geochemical anomalies (isotopic shift and platinum mineralization) again suggests simultaneous formation within a single magma chamber.

Pyroxenite Marker

Near the top of the Main Zone in both Eastern and Western limbs is an interval, referred to as the Pyroxenite Marker, characterized by a reversal in mineral compositions and a decrease in R_o (Sharpe, 1985; Cawthorn *et al.*, 1991). Above this horizon right to the top of the UZ, all analysed samples from both limbs have a uniform R_o of 0·7067 (Kruger *et al.*, 1987). The magma which produced this sequence above the Pyroxenite Marker was considered by Kruger *et al.* (1987) to be the result of complete mixing of several previously emplaced magmas with different R_o. The production of identical ratios in both limbs by mixing of several magmas is highly implausible unless the two are regarded as forming within a single magma chamber.

These four sets of observations strongly support the argument that the Eastern and Western limbs were connected (at least from the level of the Middle Group Chromitites), and that these marker horizons were originally continuous from one limb to the other.

The stratigraphic sequence in the Potgietersrus limb from the base of the MZ upwards has many similarities with that of the other two limbs, for example in having a Pyroxenite Marker interval (van der Merwe, 1976). In the Bethal lobe, only the UZ is well developed. There are, therefore, fewer unique, anomalous marker horizons in these limbs which can unequivocally be correlated with the two major limbs, and so the Potgietersrus and Bethal limbs cannot unequivocally be proven to be synchronous with the other two limbs, and they will not be included in the calculations.

Thickness

The Eastern and Western limbs attain a maximum thickness of 8 km (Fig. 2). However, there is evidence in the exposed sections for lateral thinning. In the south of the eastern limb (near Dullstroom, Fig. 11a), and in the east of the Western limb (towards Pretoria) the LZ and CZ are not developed, but are overstepped by the MZ. Hence, it is probable that in the initial filling stages, the magma chamber may have been subdivided into discrete basins with non-uniform thicknesses developed. Nevertheless, the remarkable continuity of layers, such as the Main Magnetite Layer, which can be traced for over 150 km in both the Eastern and Western lobes (Cawthorn & Molyneux, 1986), and thickness of the MZ and UZ suggest that these units were widespread and of comparable thickness everywhere. These two zones have a combined thickness of 5 km (Fig. 2). Hence an average thickness of 6 km for the entire intrusion can be regarded as a conservative estimate.

Volume estimate and emplacement rate

The above discussion illustrates that precise figures for the volume of magma in the BC cannot be obtained, but some estimates may be made. The areas delineated in Fig. 11a based on minimum extent of outcrop, metamorphic aureole, and magnetic and gravity data are 32 000 and 30 000 km^2 for Western and Eastern limbs, respectively, and a further 40 000 km^2 if the two were connected. Hence the minimum area occupied by the Bushveld magma chamber was 62 000 km^2 and probably exceeded 100 000 km^2. Using the conservative thickness of 6 km gives a volume of 372 000–600 000 km^3. However, the geochemical data for Zr, K_2O and Cr suggest that large volumes of magma have been expelled from the chamber and that the total volume of magma may have been as much as 740 000 to $1{\cdot}2 \times 10^6$ km^3. As this volume of magma was introduced in 75 000 years, the average rate of addition was between 9 and 15 km^3/year.

TERMINATION OR MIGRATION OF MAGMATIC ACTIVITY

The evidence presented above suggests that magma addition within the Eastern and Western limbs of the BC terminated abruptly with the formation of the Pyroxenite Marker. In the Western Bushveld, there are two areas where discordant bodies of Upper Zone material transgress the underlying units (Fig. 1), but rather than being due to magma addition, they are considered to be the result of redistribution of dense, iron-rich magma within the chamber (Wilson *et al.*, 1994). These observations contrast with those reported for the Duluth Complex, for example, where multiple intrusion is observed (Miller & Ripley, 1996). Each intrusion apparently discordantly cuts its predecessor, such that layering in one body is truncated by the next. This geometry may indicate migration of the feeders, and sufficiently long time intervals between each major body such that each had time to solidify and be disrupted by the next.

In the case of the Eastern and Western limbs of the BC it is argued here that they represent a single intrusion and that magma spread remarkably uniformly throughout the entire intrusion. However, it cannot be proven whether the Potgietersrus and Bethal limbs were synchronous with the Eastern and Western limbs or whether they pre- or post-dated them. The same argument applies to the largest of all the so-called satellite bodies to the BC, the Molopo Farms Complex, situated largely in Botswana (Fig. 13). It underlies an area of 13 000 km^2 and has a thickness of 3000 m (Reichhardt, 1994). Its age is about 2050 Ma (Reichhardt, 1994), making it comparable with the BC, but as the isotopic results defined an errorchron, detailed time correlation is impossible. At the present outcrop level, it is separated by at least 150 km from the Far Western limb of the BC. That gap is approximately equivalent to the entire length of all the intrusions within the Duluth Complex (Miller & Ripley, 1996). It is difficult to conclude whether magmatic activity terminated abruptly at the Pyroxenite Marker or whether it migrated. However, if it did migrate, the scale of the displacement was very considerable, such that there was no overlap between rocks derived from different centres or feeders.

CONCLUSIONS

The BC is the crystallization product of numerous injections of magma. The absence of intraplutonic quenching, and of significant changes in mineral composition

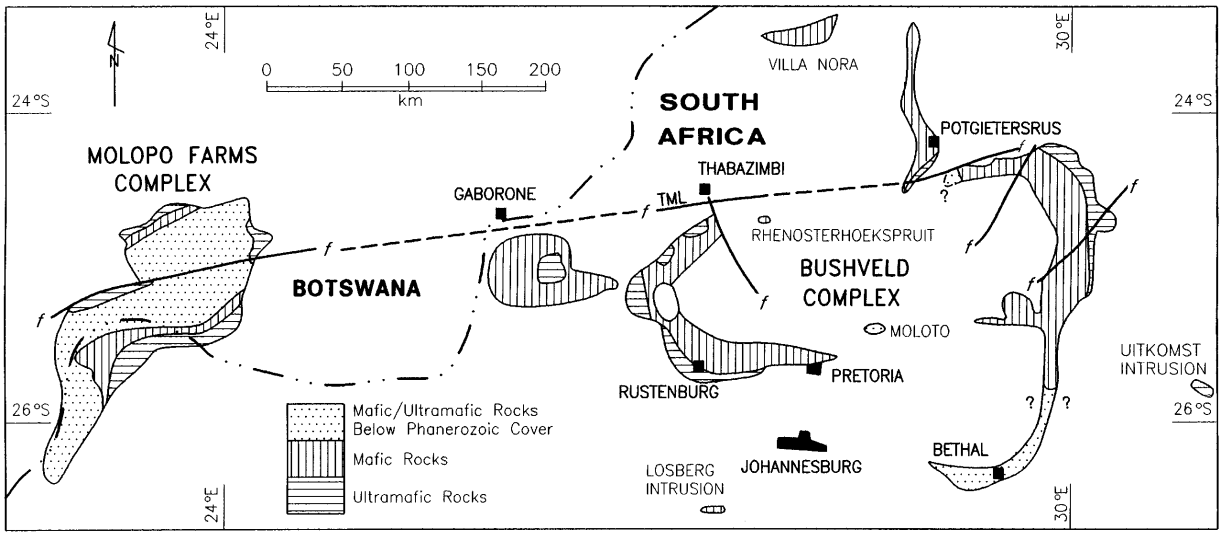

Fig. 13. Geological map showing the distribution of the Bushveld Complex and its satellites, especially the Molopo Farms Complex (Reichhardt, 1994). TML, Thabazimbi–Murchison Lineament.

within cycles and short vertical sequences, suggests that such injections are not widely separated in time. Using experimental data, the changes in mineral compositions can be converted into temperatures in the magma. Hence, the evolution of the BC can be assessed in terms of changing magma temperature, as is shown in Fig. 8. The thicknesses of magma involved can also be qualitatively modelled from a knowledge of the thickness of a particular differentiation sequence and its changes in mineral composition, again using experimental data. From the thickness of, and temperature changes in, the magma, heat flow models allow the time interval to be calculated. A numerical model has been developed for studying the cooling of magmas, which, importantly, allows for the multiple magma addition and subtraction at any time during cooling. It also allows for accumulation of solid rock at the base or top of the intrusion, stratification or mixing of magmas, the introduction of an original crustal geothermal gradient, and removal of a melt fraction from the roof.

The numerous different magma emplacement events in the BC can be identified, based on reversals in mineral compositions and sustained changes in R_o, as shown in Fig. 2 and Table 1. The model indicates that crystallization took about 200 000 years. However, the last addition of magma took place at the level of the Pyroxenite Marker near the top of the MZ only 75 000 years after the initiation of magmatism. These time estimates do not differ significantly from those calculated assuming only one injection of the entire volume of magma, but do allow for more detailed consideration of individual stages.

Differentiation of magma produces predictable sequences of mineral assemblages and mineral compositions. However, in the Eastern and Western Bushveld there are unique and distinct horizons which cannot be attributed to non-unique magma differentiation, but require additional processes, such as magma mixing. These sequences include the Middle Group Chromitites, the Upper Group Chromitite 1, the Merensky Reef, and the Pyroxenite Marker. Their remarkable similarity in both the Eastern and Western limbs strongly suggests that they formed simultaneously within a single magma chamber.

The volume of cumulate rocks in the Eastern and Western limbs can be estimated. However, the extent of the metamorphic aureole demonstrates that there was originally a larger extent to the intrusion. Furthermore, geochemical considerations indicate an originally greater volume of magma. The Cr budget for the formation of numerous chromitite layers, up to 1 m thick, demands far greater volumes of magma than are now preserved. Also, the low incompatible trace-element abundances in the UZ suggest tapping of differentiated magma. Based on these considerations the volume of magma which produced the BC may have exceeded 1×10^6 km^3, and the average rate of emplacement exceeded 9 km^3/year.

After the injection of magma at the Pyroxenite Marker, magmatism appears to have abruptly terminated or to have jumped a distance in excess of 150 km beyond the known limits of the BC, as there are no Bushveld rocks which cross-cut the UZ. Termination of magmatism may therefore have been very abrupt, rather than the

prolonged dwindling of activity as seen, for example, in the Columbia River Basalts (Hooper, 1988).

ACKNOWLEDGEMENTS

Comments on numerous drafts of this manuscript by Ian Campbell, Keith Cox, Chris Hawkesworth, James Miller, Richard Price and Richard Arculus helped to clarify its assorted concepts. The Foundation for Research Development (South Africa) is thanked for financial support to R.G.C.

REFERENCES

Barnes, S. J. (1986). The distribution of chromium among orthopyroxene, spinel and silicate liquid at atmospheric pressure. *Geochimica et Cosmochimica Acta* **50,** 1889–1909.

Barton, E. S., Alterman, W., Williams, I. S. & Smith, C. B. (1994). U–Pb zircon age from a tuff in the Campbell Group, Griqualand West Sequence, South Africa: implications for early Proterozoic rock accumulation rates. *Geology* **22,** 343–346.

Button, A. (1976). Stratigraphy and relations of the Bushveld floor in the Eastern Transvaal. *Transactions of the Geological Society of South Africa* **79,** 3–12.

Cameron, E. N. (1978). The Lower Zone of the Eastern Bushveld Complex in the Olifants River trough. *Journal of Petrology* **19,** 437–462.

Cawthorn, R. G. (1996). Re-evaluation of magma compositions and processes in the uppermost Critical Zone of the Bushveld Complex. *Mineralogical Magazine* **60,** 131–148.

Cawthorn, R. G. & Biggar, G. M. (1993). Crystallisation of titaniferous chromite, magnesian ilmenite and armalcolite in tholeiitic suites in the Karoo Igneous Province. *Contributions to Mineralogy and Petrology* **114,** 221–235.

Cawthorn, R. G. & McCarthy, T. S. (1985). Incompatible trace element behaviour in the Bushveld Complex. *Economic Geology* **80,** 1016–1026.

Cawthorn, R. G. & Molyneux, T. G. (1986). The vanadiferous magnetite deposits of the Bushveld Complex. In: Anhaeusser, C.R. & Maske, S. (eds) *Mineral Deposits of Southern Africa*. Johannesburg: Geological Society of South Africa, pp. 1251–1266.

Cawthorn, R. G., Meyer, S. P. & Kruger, F. J. (1991). Major addition of magma at the Pyroxenite Marker in the western Bushveld Complex, South Africa. *Journal of Petrology* **32,** 739–763.

Davies, G. (1980). Petrogenesis of the peripheral zone of the Rustenburg Layered Suite and associated sills between Hartbeestpoort and Buffelspoort dams, Western Bushveld Complex. Ph.D. Thesis, University of the Witwatersrand, 233 pp.

Davies, G. & Cawthorn, R. G. (1983). Mineralogical data on multiple intrusion in the Rustenburg Layered Suite of the Bushveld Complex. *Mineralogical Magazine* **48,** 469–480.

Davies, G., Cawthorn, R. G., Barton, J. M. & Morton, M. (1980). Parental magma to the Bushveld Complex. *Nature* **287,** 33–35.

du Plessis, A. & Kleywegt, R. J. (1987). A dipping sheet model for the mafic lobes of the Bushveld Complex. *South African Journal of Geology* **90,** 1–6.

du Plessis, C. P. & Walraven, F. (1990). The tectonic setting of the Bushveld Complex in Southern Africa, Part 1. Structural deformation and distribution. *Tectonophysics* **179,** 305–319.

Eales, H. V. & Cawthorn, R. G. (1996). The Bushveld Complex. In: Cawthorn, R. G. (ed.) *Layered Intrusions*. Amsterdam: Elsevier, pp. 181–229.

Eales, H. V., Marsh, J. S., Mitchell, A. A., De Klerk, W. J., Kruger, F. J. & Field, M. (1986). Some geochemical constraints upon models for the crystallisation of the upper Critical Zone–Main Zone interval, Northwestern Bushveld Complex. *Mineralogical Magazine* **50,** 567–582.

Engelbrecht, J. P. (1976). Metasediments of the Pretoria Group in the Enzelberg area, Marico District. *Transactions of the Geological Society of South Africa* **79,** 61–75.

Hattingh, P. J. (1980). The structure of the Bushveld Complex in the Groblersdahl–Lydenburg–Belfast area of the Eastern Transvaal. *Transactions of the Geological Society of South Africa* **83,** 125–133.

Hatton, C. J. (1995). Mantle plume origin for the Bushveld and Ventersdorp magmatic provinces. *Journal of African Earth Sciences* **21,** 571–577.

Hatton, C. J. & von Gruenewaldt, G. (1987). The geological setting and petrogenesis of the Bushveld chromitite layers. In: Stowe, C. W. (ed.) *Evolution of Chromium Ore Fields*. New York: Van Nostrand Reinhold, pp. 109–143.

Hooper, P. R. (1988). The Columbia River Basalt. In: Macdonald, J. D. (ed.) *Continental Flood Basalts*. Dordrecht: Kluwer Academic, pp. 1–33.

Irvine, T. N. (1970). Heat transfer during solidification of layered intrusions. I. Sheets and sills. *Canadian Journal of Earth Sciences* **7,** 1031–1061.

Jaeger, J. C. (1968). Cooling and solidification of igneous rocks. In: Hess, H. H. (ed.) *Basalts*. New York: Interscience, pp. 503–536.

Kruger, F. J. (1994). The Sr-isotopic stratigraphy of the western Bushveld Complex. *South African Journal of Geology* **97,** 393–398.

Kruger, F. J. & Marsh, J. S. (1982). Significance of $^{87}Sr/^{86}Sr$ ratios in the Merensky Cyclic Unit of the Bushveld Complex. *Nature* **298,** 53–55.

Kruger, F. J., Cawthorn, R. G. & Walsh, K. L. (1987). Strontium isotope evidence against magma addition in the Upper Zone of the Bushveld Complex. *Earth and Planetary Science Letters* **84,** 51–58.

Lee, C. A. (1981). Post-deposition structures in the Bushveld Complex mafic sequence. *Journal of the Geological Society, London* **138,** 327–341.

Lee, C. A. & Butcher, A. R. (1990). Cyclicity in the Sr-isotopic stratigraphy through the Merensky and Bastard Reef Units, Atok Section, Eastern Bushveld Complex. *Economic Geology* **85,** 877–883.

Lipin, B. R. (1993). Pressure increases, the formation of chromite seams, and the development of the Ultramafic Series in the Stillwater Complex, Montana. *Journal of Petrology* **34,** 955–976.

Marlow, A. G. & van der Merwe, M. J. (1977). The geology and potential economic significance of the Malope area, north-eastern Bushveld Complex. *Transactions of the Geological Society of South Africa* **80,** 117–124.

Miller, J. D., Jr & Ripley, E. M. (1996). The layered intrusions of the Duluth Complex, Minnesota, USA. In: Cawthorn, R. G. (ed.) *Layered Intrusions*. Amsterdam, Elsevier, pp. 257–302.

Mitchell, A. A. (1986). The petrology, mineralogy and geochemistry of the Main Zone of the Bushveld Complex, at Rustenburg Platinum Mines, Union Section. Ph.D. Thesis, Rhodes University, South Africa, 122 pp.

Mitchell, A. A. (1990). The stratigraphy, petrography and mineralogy of the Main Zone of the Northwestern Bushveld. *South African Journal of Geology* **93,** 818–831.

Molyneux, T. G. (1974). A geological investigation of the Bushveld Complex in Sekhukhuneland and part of the Steelpoort valley. *Transactions of the Geological Society of South Africa* **77,** 329–338.

Molyneux, T. G. & Klinkert, P. S. (1978). A structural interpretation of part of the eastern mafic lobe of the Bushveld Complex and its surroundings. *Transactions of the Geological Society of South Africa* **81,** 359–368.

Murck, B. W. & Campbell, I. H. (1986). The effects of temperature, oxygen fugacity and melt composition on the behaviour of chromium in basic and ultrabasic melts. *Geochimica et Cosmochimica Acta* **50,** 1871–1887.

Reichhardt, F. J. (1994). The Molopo Farms Complex, Botswana: history, stratigraphy, petrography, petrochemistry and Ni–Cu–PGE mineralization. *Exploration and Mining Geology* **3,** 263–284.

Sharpe, M. R. (1981). The chronology of magma influxes to the eastern compartment of the Bushveld Complex as exemplified by its marginal border groups. *Journal of the Geological Society, London* **138,** 307–326.

Sharpe, M. R. (1985). Strontium isotope evidence for preserved density stratification in the Main Zone of the Bushveld Complex. *Nature* **316,** 119–126.

South African Commission on Stratigraphy (1980). *Stratigraphy of South Africa. Geological Survey of South Africa, Handbook 8*. Pretoria: Geological Survey of South Africa, p. 690.

Snyder, D., Carmichael, I. S. E. & Wiebe, R. A. (1993). Experimental study of liquid evolution in an Fe-rich, layered mafic intrusion: constraints of Fe–Ti oxide precipitation on the T–fO_2 and T–p paths of tholeiitic magmas. *Contributions to Mineralogy and Petrology* **113,** 73–86.

Tegner, C., Wilson, J. R. & Brooks, C. K. (1993). Intraplutonic quenching in the Kap Edvard Holm layered gabbro complex, East Greenland. *Journal of Petrology* **34,** 681–710.

Teigler, B. & Eales, H. V. (1996). The Lower and Critical Zones of the western limb of the Bushveld Complex as intersected by the Nooitgedagt boreholes. *Geological Survey of South Africa, Bulletin* **111,** 126 pp.

Toplis, M. J. & Carroll, M. R. (1995). An experimental study of the influence of oxygen fugacity on Fe–Ti oxide stability, phase relations and mineral–melt equilibria in ferro-basaltic systems. *Journal of Petrology* **36,** 1137–1170.

van der Merwe, M. J. (1976). The layered sequence of the Potgietersrus limb of the Bushveld Complex. *Economic Geology* **71,** 1337–1351.

von Gruenewaldt, G. (1970). On the phase change orthopyroxene–pigeonite and the resulting textures in the Main and Upper Zones of the Bushveld Complex in the Eastern Transvaal. *Geological Society of South Africa, Special Publication* **1,** 67–73.

von Gruenewaldt, G. (1973*a*). The Main and Upper Zones of the Bushveld Complex in the Roossenekal area, eastern Transvaal. *South African Journal of Geology* **76,** 207–227.

von Gruenewaldt, G. (1973*b*). The modified differentiation index and the modified crystallisation index as parameters of differentiation. *Transactions of the Geological Society of South Africa* **76,** 53–61.

Wager, L. R. & Brown, G. M. (1968). *Layered Igneous Rocks*. Edinburgh: Oliver and Boyd, 588 pp.

Walraven, F. (1987). Geochronological and isotopic studies of Bushveld Complex rocks from the Fairfield borehole at Moloto, northeast of Pretoria. *South African Journal of Geology* **90,** 352–360.

Walraven, F. & Darracott, B. W. (1976). Quantitative interpretation of a gravity profile across the Western Bushveld Complex. *Transactions of the Geological Society of South Africa* **79,** 22–26.

Walraven, F., Armstrong, R. A. & Kruger, F. J. (1990). A chronostratigraphic framework for the north–central Kaapvaal Craton, the Bushveld Complex and Vredefort structure. *Tectonophysics* **171,** 23–48.

Wilson, J. R., Cawthorn, R. G., Kruger, F. J. & Grundvig, S. (1994). A major unconformity in the western Bushveld Complex: the northern 'gap'. *South African Journal of Geology* **97,** 462–472.

Yang, H.-J., Kinzler, R. J. & Grove, T. L. (1996). Experiments and models of anhydrous, basaltic olivine–plagioclase–augite saturated melts from 0·001 to 10 kbar. *Contributions to Mineralogy and Petrology* **124,** 1–18.